University of Massachusetts Amherst

ScholarWorks@UMass Amherst

Biology Department Faculty Publication Series

Biology

2004

Disorganization of cortical microtubules stimulates tangential expansion and reduces the uniformity of cellulose microfibril alignment among cells in the root of Arabidopsis

TI Baskin

GTS Beemster

JE Judy-March

F Marga

Follow this and additional works at: https://scholarworks.umass.edu/biology_faculty_pubs

Part of the Biology Commons

Disorganization of Cortical Microtubules Stimulates Tangential Expansion and Reduces the Uniformity of Cellulose Microfibril Alignment among Cells in the Root of Arabidopsis[1]

Tobias I. Baskin[2]*, Gerrit T.S. Beemster[3], Jan E. Judy-March, and Françoise Marga

Division of Biological Sciences, University of Missouri, Columbia, Missouri 65211

To test the role of cortical microtubules in aligning cellulose microfibrils and controlling anisotropic expansion, we exposed *Arabidopsis thaliana* roots to moderate levels of the microtubule inhibitor, oryzalin. After 2 d of treatment, roots grow at approximately steady state. At that time, the spatial profiles of relative expansion rate in length and diameter were quantified, and roots were cryofixed, freeze-substituted, embedded in plastic, and sectioned. The angular distribution of microtubules as a function of distance from the tip was quantified from antitubulin immunofluorescence images. In alternate sections, the overall amount of alignment among microfibrils and their mean orientation as a function of position was quantified with polarized-light microscopy. The spatial profiles of relative expansion show that the drug affects relative elongation and tangential expansion rates independently. The microtubule distributions averaged to transverse in the growth zone for all treatments, but on oryzalin the distributions became broad, indicating poorly organized arrays. At a subcellular scale, cellulose microfibrils in oryzalin-treated roots were as well aligned as in controls; however, the mean alignment direction, while consistently transverse in the controls, was increasingly variable with oryzalin concentration, meaning that microfibril orientation in one location tended to differ from that of a neighboring location. This conclusion was confirmed by direct observations of microfibrils with field-emission scanning electron microscopy. Taken together, these results suggest that cortical microtubules ensure microfibrils are aligned consistently across the organ, thereby endowing the organ with a uniform mechanical structure.

How do plants build organs with specific and heritable shapes? A part of the answer to this question lies in the control of growth. It is not growth rate per se that is crucial for morphogenesis but the directionality of growth. If growth rate were the same in all directions, i.e. isotropic, plant organs would be spherical; organs attain shapes other than spherical because their component cells grow at different rates in different directions, i.e. anisotropically. Understanding how cells control the anisotropy of their expansion is essential for understanding morphogenesis.

Expansion anisotropy is characterized by the direction in which the maximal growth rate occurs and by the degree to which the maximum differs from the minimum. The direction of maximal expansion rate is known to be controlled by the direction of net alignment of cellulose microfibrils. Within a growing cell wall, microfibrils are aligned, on average, perpendicularly to the direction of maximal expansion rate, and the aligned cellulose microfibrils confer a mechanical anisotropy on the cell wall, which translates into expansion anisotropy (Green, 1980; Taiz, 1984). The wall can be considered a composite material with strong, rod-shaped particles (microfibrils) embedded in a compliant matrix. Such materials deform perpendicular to the rod's long axis more readily than parallel, giving rise to the anisotropic yielding behavior of the cell wall (Mark, 1967).

In contrast to the direction of maximal expansion rate, it is not known whether the degree of anisotropy is also controlled by the alignment of microfibrils. The direction of maximal expansion rate can be safely inferred for a straight-growing cylindrical organ, such as a root; however, there is no way to know the degree of anisotropy without measuring it. Surprisingly, there have been few published measurements of growth anisotropy in plant organs. Those that have been made show that the degree of anisotropy differs with position, species, and treatment (Erickson, 1966; Silk and Abou Haidar, 1986; Liang et al., 1997). One of our aims here was to quantify the spatial profiles of expansion in length and radius and compare them to the underlying profile of microfibril alignment. In that way, microfibril alignment might be discovered to specify the degree of growth anisotropy.

[2] Present address: Biology Department, University of Massachusetts, Amherst, MA 01003.

[3] Present address: Department of Plant Systems Biology, Flanders Interuniversity Institute for Biotechnology (VIB), Ghent University, Technologiepark 927, B–9052 Ghent, Belgium.

* Corresponding author; e-mail baskin@bio.umass.edu; fax 413–545–3243.

In cylindrical organs, rates of expansion perpendicular to elongation (i.e. radial or tangential expansion) are generally small and difficult to quantify. To increase the magnitude of tangential expansion rate, we inhibited the function of cortical microtubules partially. In contrast to inhibiting microtubules totally, which gives rise to more or less isotropic expansion, we hypothesized that inhibiting them partially would stimulate tangential expansion modestly, making it easier to measure, but not enough to make expansion isotropic. The biochemistry of interaction between the microtubule inhibitor, oryzalin, and plant tubulin has been well characterized (Hugdahl and Morejohn, 1993) and partial inhibition at low concentration minimizes the possibility of nonspecific effects. We used low concentrations of oryzalin, which allowed growth to continue at a reduced but virtually steady rate for several days, and quantified profiles of longitudinal and tangential expansion rate and, concomitantly, the spatial profile of microfibril alignment.

The use of low concentrations of a microtubule inhibitor also allows us to address the question of whether cellulose microfibrils are aligned by cortical microtubules, which was suggested when microtubules were discovered (Ledbetter and Porter, 1963; Hepler and Newcomb, 1964) but has lately become controversial (Wasteneys and Galway, 2003). A role for microtubules in aligning microfibrils is supported by a substantial body of evidence (Baskin, 2001; Burk and Ye, 2002; Gardiner et al., 2003). Nevertheless, some have argued that the parallelism between microtubules and microfibrils represents a correlated response to an unknown polarizing principle rather than a causal relation (Emons et al., 1992). Furthermore, microfibril alignment by microtubules is at odds with some recent results. For example, most cells in the maturation zone of the water-stressed maize (*Zea mays*) root have microtubule arrays in right-handed helices but microfibrils in left-handed helices (Baskin et al., 1999). Similarly, the Arabidopsis (*Arabidopsis thaliana*) mutant, *microtubule organization 1* (*mor1*), has aberrant microtubule arrays but apparently unaltered microfibril alignment (Himmelspach et al., 2003; Sugimoto et al., 2003).

We hypothesized that in material treated with low concentrations of a microtubule inhibitor, a substantial population of cortical microtubules would remain, and, if so, then their organization could be correlated with that of the microfibrils. This would make a useful contrast to *mor1*, assuming that chemical inhibition of microtubule polymerization affects cortical microtubules differently than does genetic ablation of the MOR1 protein. Hence, the contention that microtubules align microfibrils would either be further refuted or instead supported with a counterexample.

For this work, we used Arabidopsis roots. The small size of the root facilitates cytological analysis and, surprisingly, is also convenient for growth analysis (Beemster and Baskin, 1998). Furthermore, this species in general and the root in particular have been used in much recent work bearing on the role of microtubules

in aligning microfibrils. To examine microtubules, we used ambient-pressure cryofixation, maximizing the chances of preserving labile microtubules induced by oryzalin. Cryofixing multicellular samples is customarily done at high pressure to avoid ice crystal damage; however, for light microscopy, it has been shown that ambient-pressure cryofixation of Arabidopsis roots performs better than chemical fixation by several criteria (Baskin et al., 1996).

We report evidence suggesting that the degree of anisotropy may be controlled by differences in the net alignment among microfibrils in neighboring cells. Additionally, we report that microtubules have a role in orienting microfibrils; however, rather than influencing cellulose alignment on the subcellular scale, the cortical array appears to act through imposing a uniform order on microfibril alignment among neighboring cells in the root.

RESULTS

Determination of Suitable Inhibitor Concentrations

To inhibit microtubule function partially, we chose oryzalin, because its interaction with plant tubulin has been well characterized (Hugdahl and Morejohn, 1993). Nevertheless, with any inhibitor, there may be nonspecific effects; therefore, we compared oryzalin to microtubule inhibitors with other chemical structures (Vaughn and Lehnen, 1991). One-week-old seedlings were transplanted onto plates containing an inhibitor, exposed for 2 d, and root elongation rate over the 2nd d of treatment and diameter at the end of treatment were measured. Two compounds, clorpropham and nocodazole, inhibited elongation at lower concentrations than needed to stimulate radial expansion (Fig. 1), possibly because they affected mitotic microtubules more actively than cortical ones (Hoffman and Vaughn, 1994). The remaining compounds had the same threshold for inhibiting elongation and stimulating radial expansion. The compounds differed in the extent of swelling and in the steepness of the dose-response curve. Oryzalin, like most of the compounds, increased diameter at least 3-fold and had a saturating concentration about 10 times the threshold. Colchicine and RH-4032 (Young and Lewandowski, 2000) increased diameter 5-fold and had a steeper dose-response curve, which suggests that these two compounds may be preferable for work at high doses. We selected 170 nM oryzalin as the low dose (just above threshold) and 300 nM as the moderate dose.

Spatial Distribution of Longitudinal and Tangential Relative Expansion Rate

We examined root elongation over time for seedlings transplanted onto control medium or medium containing 170 nM or 300 nM oryzalin (Fig. 2). In controls, root elongation rate accelerated, as previously reported (Beemster and Baskin, 1998). Roots on
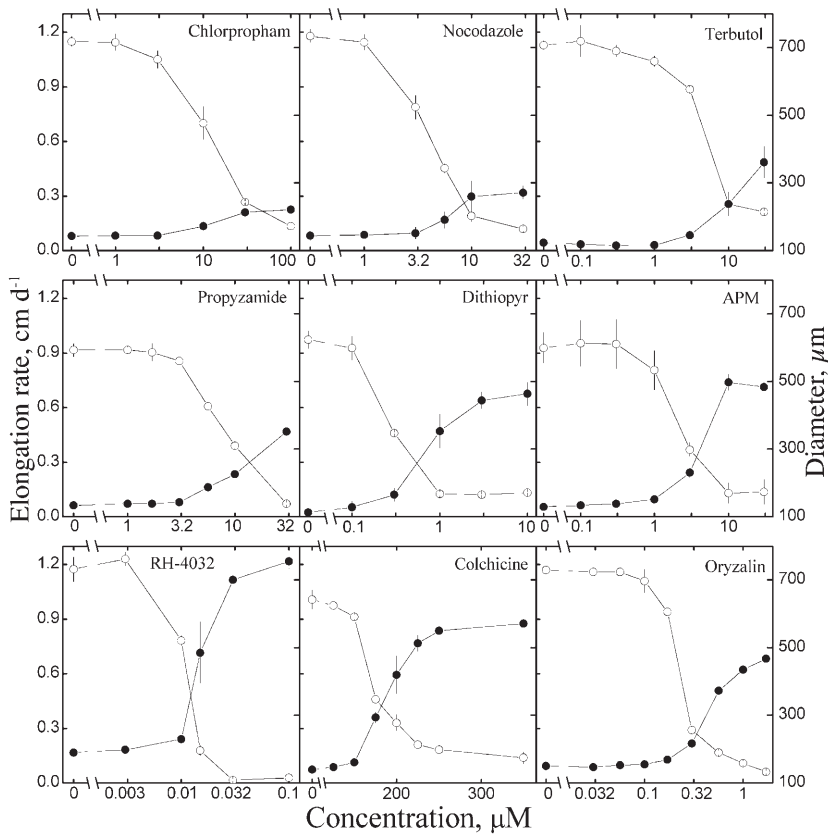
Figure 1. Comparison of the effects of microtubule inhibitors on Arabidopsis root growth. Seedlings were transferred to inhibitor plates and elongation rate (white circles) measured over the second 24 h of treatment and diameter (black circles) measured at the end of that period. Symbols plot mean ± SE from three replicate experiments or in most cases from three replicate plates. Concentration is plotted logarithmically except for colchicine. Control diameter and elongation rate differed among the experiments for unknown reasons.

170 nM oryzalin reached a steady-state growth rate after 1 d, which continued for at least several days (longer term experiments not shown). Roots on 300 nM oryzalin were considerably inhibited but nevertheless continued to elongate at a finite rate for more than 5 d. For all following experiments, we fixed drug-treated
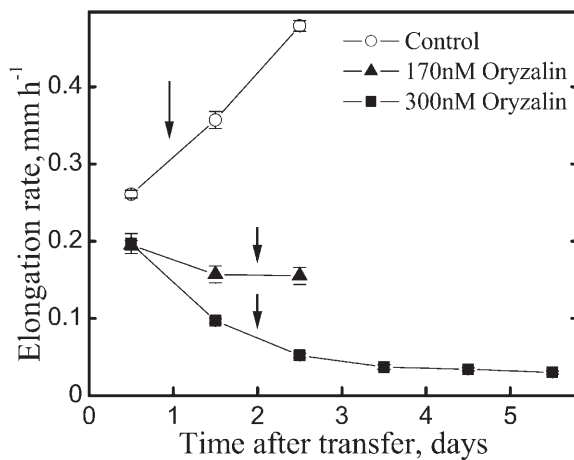

Figure 2. Time course of root elongation following transfer to oryzalin or control plates. Seven-day-old seedlings were transferred at time zero and elongation rate measured at 24 h intervals and plotted at the midpoint time. Arrows show the times when samples were fixed. Symbols plot mean ± SE of three plates.

seedlings 2 d after transfer, when elongation rate was steady or nearly so, and control seedlings 1 d after transfer, to have roots that were shorter and hence easier to handle (Fig. 2, arrows).

We quantified the spatial distribution of relative expansion kinematically (Liang et al., 1997; Beemster and Baskin, 1998). Sample images from the analysis are shown in Figure 3. The black spots are the graphite particles used for measurement. Roots on oryzalin were swollen and root hairs differentiated close to the tip. On 300 nM oryzalin, roots were less swollen than roots grown on a saturating concentration, 1.7 μM, which have almost no microtubules and which cease growth by 2 d of exposure (Baskin et al., 1994).

The spatial profile of relative elongation rate is shown in Figure 4 (top). Oryzalin truncated the growth zone progressively with concentration. Surprisingly, elongation rates in the apical portion of the root were indistinguishable among the three treatments. In the initial 200 μm or so of the profile (which is mainly root cap) rates differed, probably because the ends of the data set are prone to curve-fitting errors (Beemster and Baskin, 1998).

Relative tangential expansion rate quantifies the rate of expansion of the root's circumference. In controls, tangential expansion rate was low, 1% h^{-1} or less, in the first 400 μm of the root, and then became negative for the next 500 μm and possibly farther (Fig. 4). Negative rates occur because root diameter decreases,
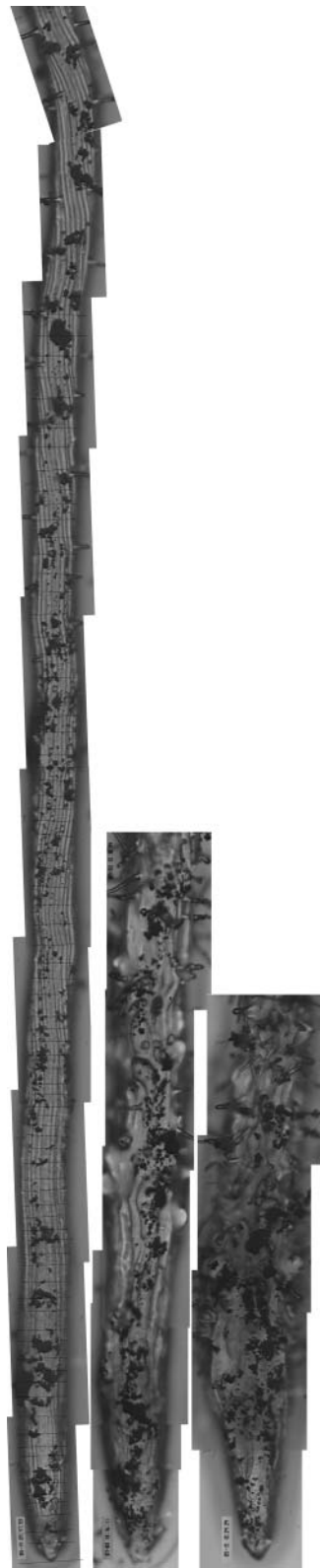
Figure 3. Bright-field, composite micrographs of roots used for growth analysis, sampled as described for Figure 2. Left image shows control, center shows 170 nM oryzalin, and right shows 300 nM oryzalin. Black spots on the roots are the graphite particles used to measure local velocities. Roughly horizontal black lines on control were applied

starting at about the location where cell length begins to increase markedly. Even where tangential expansion rates were positive, they were much smaller than elongation rates, showing that growth was highly anisotropic throughout the growth zone, including the meristem. Oryzalin promoted tangential expansion, with the maximal rate occurring a little basal of the relative elongation rate maximum. Interestingly, maximal tangential rate was the same on 300 and 170 nM oryzalin, but moved apically under the higher dose. The apical shift led to thicker roots because cells at the more apical locations moved more slowly than those more basal; therefore on 300 nM oryzalin, cells experienced the maximal tangential expansion rate for a longer time and thus swelled to a greater extent. Even on 300 nM oryzalin, growth remained anisotropic, but the degree of anisotropy was less than at 170 nM and much less than that of controls.

Patterns of Microtubule Organization

To examine microtubules, roots were cryofixed at the times indicated by Figure 2, freeze-substituted, embedded, sectioned, and stained with antitubulin (Baskin et al., 1996). Fluorescence was dim in the maturation zone and microtubules there were not examined. In the growth zone, oryzalin appeared to affect microtubules similarly in all tissues. In dividing cells, preprophase bands and phragmoplasts were often misaligned. Additionally, cell shapes were distorted, as if from the deposition of cell walls at oblique angles (see below). Cortical arrays in control were dense and transverse to the root's long axis; whereas on oryzalin, the cortical array appeared to contain fewer microtubules and to be partially disorganized (Fig. 5). Particularly on 300 nM oryzalin, microtubules appeared thicker and shorter, but light microscopy has insufficient resolution to determine length or bundling unambiguously (Williamson, 1991).

We quantified the angular distribution of microtubules for cortex and epidermis (Fig. 6). The frequency plots divided angles into 10-degree classes, with 90° representing transverse. The angular distribution of cortical microtubules in control was sharp and centered on 90° for the first 900 μm from the quiescent center, coinciding with increasing relative elongation rate (Fig. 4). With greater distance, where elongation rate decreases, 90° orientation was replaced gradually by a bimodal distribution, with peaks at 45° and 135°, indicating oblique microtubules (Fig. 6). Oblique angles occur where microtubule arrays are helical, and even though the helices are nearly all right-handed (Liang et al., 1996; Thitamadee et al., 2002), orientations of 45° and 135° are seen equally because sectioning presents views of the helices from inside and outside. On oryzalin, the means of the

manually to aid measurement (see Beemster and Baskin, 1998). Control root is approximately 150 μm in diameter.
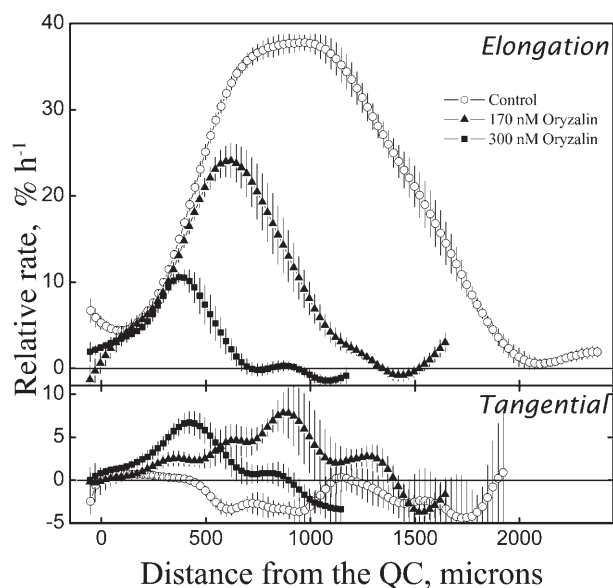
Figure 4. Spatial profiles of relative elongation rate (top) and tangential expansion rate (bottom). Data plot mean ± SE (when larger than the symbol) for 5 replicate roots. QC, Quiescent center. Material was taken for growth analysis at the times given in Figure 2.

distributions were consistently 90° but the distributions were flattened, particularly at 300 nM, and the reorientation to oblique angles was minimal or absent.

Patterns of Microfibril Orientation

To examine cellulose microfibrils, we used polarized-light microscopy. To ensure congruence of the data sets, alternate sections were collected for analysis of microtubules and microfibrils. As described in "Materials and Methods," the quantitative polarized-light attachment produces a pair of images, one showing retardance and the other optical azimuth of the retarding elements. We quantified both parameters for epidermal and cortical cell walls lying parallel to the section plane (i.e. longitudinal-radial cell walls).

Retardance images reveal cell shape clearly, highlighting the misplacement of cell walls on oryzalin (Fig. 7). The misaligned cell walls meant that in oryzalin-treated material there was less cell wall lying parallel to the section plane available for measurement; nevertheless, some was present and virtually all suitable areas were sampled per image (see "Materials and Methods"). Retardance of controls reached a peak in the meristem and then gradually declined (Fig. 8A). On oryzalin, retardance became significantly greater than control; this happened for 170 nM beyond about 750 μm from the quiescent center and for 300 nM beyond about 250 μm. The locations where retardance surpassed the control level also had elevated rates of tangential expansion; therefore, increased tangential expansion, and hence root swelling on oryzalin, was accompanied by there being denser or better-aligned microfibrils. In contrast to retardance, the average azimuth was approximately 90° for all positions and

did not differ significantly among treatments (Fig. 8B). This appears to indicate that microfibril directionality was unaltered despite the pronounced deterioration in microtubule organization.

However, Figure 8, A and B, plot means and SEs. These errors reflect the variability among roots. We then assessed the variability among measurements by looking at the SDs, which were obtained for each root, and averaged (Fig. 8, C and D). The deviations for the retardance data tended to be proportional to the retardance values themselves, a scaling behavior that typifies many parameters. In contrast, the deviations for the azimuth data differed; compared to controls, deviations for the oryzalin-treated roots were larger and, what's more, appeared to increase at around the location where tangential expansion rate increased. These data show that although the net orientation among all microfibrils remained transverse (Fig. 8B), local regions of cell wall had divergent microfibril orientation. Similarly, saturating oryzalin for 24 h altered microfibril orientation globally but not locally (Sugimoto et al., 2003).

To confirm the polarized-light data, we examined the innermost layer of the cell wall with field-emission scanning electron microscopy (FESEM). Care was taken to collect images of cortical or epidermal cells from within the growth zone (within 1,500 μm from the quiescent center in controls, 1,000 μm for 170 nM oryzalin, 600 μm for 300 nM). Cell walls in control roots had microfibrils with uniformly transverse orientation (Fig. 9, A and B); however, cells on 170 nM (Fig. 9, C and D) and 300 nM oryzalin (Fig. 9, E and F) often had microfibril alignments that deviated from the transverse. Although microfibril alignment was usually coherent at the level of a single image, occasionally
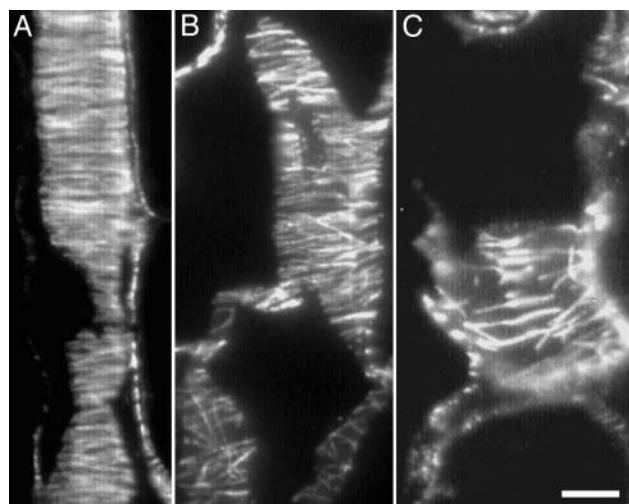

Figure 5. Fluorescence micrographs of cortical microtubules in root cortex cells within the elongation zone, representative of the treatments. Methacrylate sections stained with an antitubulin antibody. The root's long axis is parallel to the long side of the page. Material was sampled according to Figure 2. A, Control; B, 170 nM oryzalin; C, 300 nM oryzalin. Bar represents 10 μm.

Figure 6. Frequency distributions of microtubule angle as a function of position. The root's long axis is defined as 0°. Angles were binned in 10° intervals, starting at 0° and plotted at the midpoint. Distances of the measured arrays were binned in 100-μm intervals, starting at the quiescent center or, for controls, at 100 μm from there. Distributions reflect pooled data from six roots, with 5,600 to 8,200 microtubules per treatment. Symbols are shown only on the apical-most distributions. Each distribution was normalized as percent of its maximum and successive distributions are displaced on the ordinate by 10%. Data are for cortex and epidermis. Material sampled according to Figure 2.
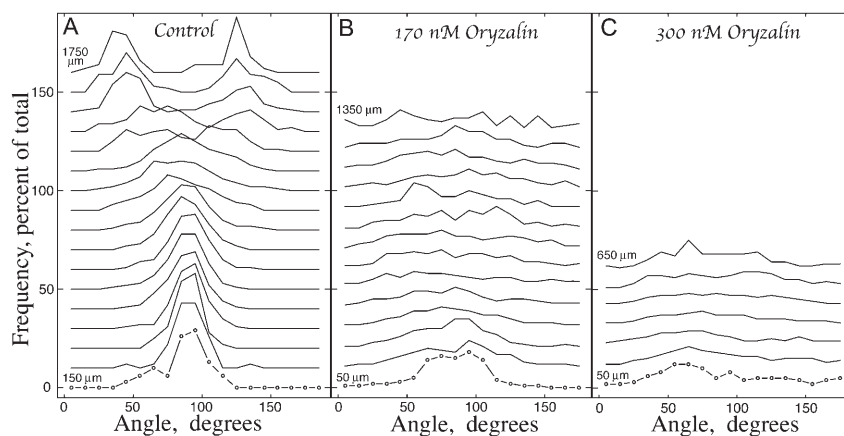
in the 300 nM samples, cell walls had bands of divergent microfibrils (Fig. 9F). As described in "Materials and Methods," the average degree of alignment among microfibrils, as well as their net angular orientation, was quantified by means of their fast Fourier transforms (FFTs; Table I). The eccentricity of the transforms at three spatial frequencies (at about the size of the prominent fibrillar structures in the micrographs) was essentially the same for the treatments, indicating that there was little difference in the angular divergence among the microfibrils (divergence would tend to make the transform less eccentric). On the other hand, the angle defined by the major axis of the ellipse and the long axis of the root was significantly more variable on oryzalin than in controls. These results support the polarized light data; microfibril orientation in roughly 1 μm^2 patches was not degraded on oryzalin, but orientations in different cells were less consistent.

DISCUSSION

Growth Patterns

To our knowledge, this is the first report quantifying tangential expansion rates for the Arabidopsis root,
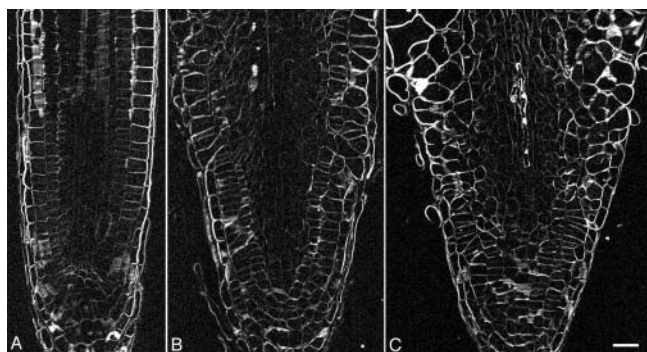

Figure 7. Polarized-light micrographs (retardance images) of the root tip. Methacrylate sections of material sampled according to Figure 2. A, Control; B, 170 nM oryzalin; C, 300 nM oryzalin. Bar represents 20 μm.

and for the root of any species exposed to a microtubule inhibitor. For calculation, we assumed steady-state growth, even though diameter increases with time (van der Weele et al., 2000). This gives rise to a time-dependent expansion rate, without which tangential rates are underestimated. By measuring the spatial profile of diameter on days 1, 2, and 3, we found that the term is about 0.3% h^{-1} for controls, slightly larger for 170 nM, and smaller for 300 nM oryzalin. Importantly, the term is essentially the same at all positions in the growth zone. Spatial constancy was also reported for the time-dependent change in the diameter of the well-watered maize root (Liang et al., 1997). Therefore, neglecting the time-dependent term underestimates tangential rate inconsequentially.

In the control, tangential rates peak at about 1% h^{-1} in the meristem and fall to about −4% h^{-1} in the elongation zone (Fig. 4). Negative expansion rates of any kind are unusual, reported previously for regions of the shoot apical meristem in folds between emerging primordia (Kwiatkowska and Dumais, 2003) and for the concave side of bending organs, where the strong growth of the convex side may compress the weakly growing concave side. In a straight-growing organ like the root, differential stresses between inner and outer tissues could conceivably cause tangential shrinkage. Another potential cause is the loss of the lateral root cap, which sheathes the root around the apex but disappears at about the location where shrinkage occurs.

Expansion throughout the Arabidopsis root's growth zone, including the meristem, is anisotropic, although the degree of anisotropy varies with position. Some authors have observed the roughly isodiametric cell shapes in the Arabidopsis root meristem and have mistakenly concluded that expansion there is isotropic (e.g. Bichet et al., 2001). Cell shape is formed by division as well as expansion; therefore, static images of meristem cell shape reveal nothing about expansion anisotropy (Green, 1976; Baskin and Beemster, 1998).

Microtubule inhibitors are often thought to reduce elongation because they stimulate lateral expansion, as if the rate of cell wall area expansion were constant.
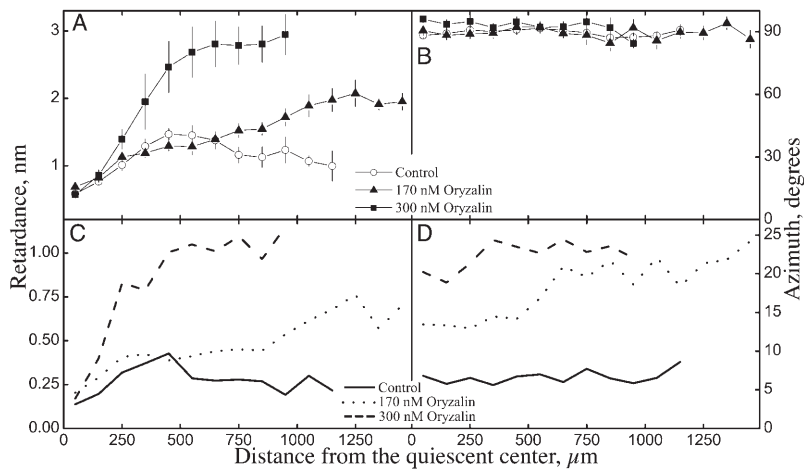
Figure 8. Retardance (A and C) and azimuth (B and D) as a function of position. Data in A and B plot the mean ± SE for four (control and 300 nM oryzalin) or five roots. For C and D, the SDs for the 20 to 80 measurements at each position were obtained for each root, averaged over the roots, and plotted without symbols. Data are for cortex and epidermis. Material was sampled according to Figure 2.

This explanation is untenable here because, for example, at 300 μm from the quiescent center, elongation rates for the three treatments are identical but tangential expansion rates differ by a factor of 5 (Fig. 4). Instead, microtubule inhibition appears to affect elongation and tangential expansion by different mechanisms. Elongation rate is truncated apically, as also reported over time for wild-type roots responding to saturating oryzalin and for *mor1* roots responding to a shift in temperature (Sugimoto et al., 2003). Because elongation zones are truncated apically when a root responds to deficits of water (Sharp et al., 1988) and phosphorus (Ma et al., 2003), we postulate that the truncation of the elongation rate profile reflects a response to stress, whereas the stimulation of tangential

expansion is specific to the disruption of microtubule function.

Microtubule Organization

Hoffman and Vaughn (1994) reported that low doses of various microtubule inhibitors, including oryzalin, disorganize all classes of microtubule array in oat (*Avena sativa*) roots, although their paper focused on mitotic arrays. Here, in addition to disorganizing the cortical array, low oryzalin prevented cortical microtubule reorientation from transverse to oblique and led to misplaced preprophase bands, phragmoplasts, and cell walls. In fact, aberrant phragmoplasts and
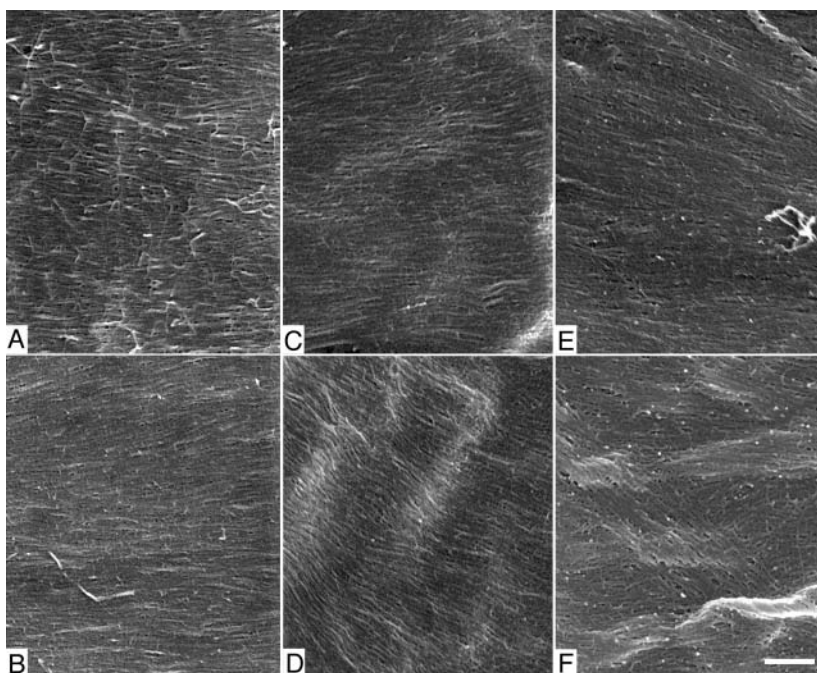
Figure 9. FESEM micrographs of the innermost cell wall layer taken within the growth zone. A and B, Control; C and D, 170 nM oryzalin; E and F, 300 nM oryzalin. The long axis of the root is parallel to the long side of the page. For the oryzalin treatments, images are representative of least affected (upper) and most affected (lower) cell walls. All images are from cortex or epidermis. Material was sampled according to Figure 2. Bar represents 250 nm.

Table I. *Analysis of orientation parameters from FESEM images of cell walls*

These parameters were obtained from the Fourier transform, as described in "Materials and Methods." Number of cells examined: 20 (control), 14 (170 nM oryzalin), and 12 (300 nM oryzalin).

Spacing, nm	Eccentricity, Mean ± SD		
	Control	170 nM Oryzalin	300 nM Oryzalin
18.6	0.92 ± 0.12	0.93 ± 0.09	0.87 ± 0.09
23.75	0.91 ± 0.13	0.96 ± 0.06	0.94 ± 0.05
32.7	0.96 ± 0.05	0.94 ± 0.03	0.94 ± 0.07
	Angle, Degrees, Mean ± SD		
18.6	0 ± 13	2 ± 19	12 ± 28
23.75	−1 ± 16	2 ± 30	5 ± 25
32.7	0 ± 17	7 ± 36	−2 ± 30

misplaced cell walls are seen frequently in roots exposed to microtubule inhibitors (Ennis, 1948; Hardham and Gunning, 1980; Holmsen and Hess, 1985; Cleary and Hardham, 1988; Galatis and Apostolakos, 1991; Hoffman and Vaughn, 1994). Given that the preprophase band helps to determine the placement of the cell plate (Mineyuki, 1999), it is reasonable that misaligned preprophase bands be followed by misaligned cell walls. We hypothesize that disorder in both preprophase and cortical arrays arises from decreased microtubule stability. Regardless of mechanism, these results highlight the importance of microtubules for the alignment of the cell plate.

Conceivably, the misdirected cross walls impair the plant's ability to align cellulose microfibrils, but evidence suggests otherwise. The disposition of cross walls appears to have little influence on anisotropic expansion and microfibril alignment. For example, the *tangled* mutant of maize has aberrant cross walls but essentially normal leaf shape (Smith et al., 2001); similarly, in two radially swollen mutants of Arabidopsis, cell wall placement is reminiscent of the oryzalin treatment studied here but swelling is unchanged when the production of the misaligned cell walls is inhibited (Wiedemeier et al., 2002).

Microfibril Organization

On oryzalin, the increase in retardance compared to control, particularly striking for 300 nM, indicates that microfibrils become better organized or there are more microfibrils per unit area of cell wall (or both). The reason for increased retardance is unknown. In principle, an increased retardance within the basal part of the elongation zone in controls could move apically under oryzalin; however, such an increase was absent from controls processed on other occasions where the sections included the basal part of the elongation zone. Alternatively, oryzalin could enhance microfibril self-assembly, but, if so, then one would expect to see evidence of this in FESEM images, which, as analyzed through the Fourier transforms, are indistinguishable among the treatments, except in the orientation of the

transform. Finally, retardance may have increased because the so-called multi-net reorientation decreased. Efficient multi-net rotation of transverse microfibrils depends on highly anisotropic expansion (Erickson, 1980; Preston, 1982); for 300 nM oryzalin, where the increase of retardance is largest, expansion is nearly isotropic. Therefore, the increased retardance could reflect decreased multi-net reorientation in older layers of the cell wall, but modeling will be required to assess this explanation.

Microtubule-Microfibril Syndrome

We show here that cortical microtubules are dispensable for microfibril alignment locally but not globally, a conclusion that has been reached previously (Baskin, 2001; Sugimoto et al., 2003). By local we refer to subcellular regions, 10 μm^2 or less, an area typical of the polarized-light samples and larger than the area sampled in FESEM (<1 μm^2). By global, we refer to whole cells or groups of cells. Sampling within cells in polarized light was precluded because a cell rarely had more than one area suitable for measuring. In FESEM, in principle, different parts of the same cell could have been compared; however, for the oryzalin-treated roots, cell walls tended to wrinkle and the entire cell wall area was rarely useful. Furthermore, the FESEM technique is difficult and few samples were processed successfully, particularly for 300 nM oryzalin. Based on images we did obtain, on 300 nM oryzalin, the breakdown of coherent microfibril alignment can occur within the same cell (Fig. 9F); but whether the breakdown is consistently within or between cells will require further investigation.

On the local scale, for diffuse-growing higher plant cells, microtubule disruption rarely leads to misaligned microfibrils (Baskin, 2001); however, nearly all previous experiments assessed microfibril alignment visually. In contrast, Sugimoto et al. (2003) measured the angles of individual microfibrils in FESEM and here we quantified microfibril alignment in both FESEM and polarized-light microscopy. That local microfibril alignment does not require microtubules is thus demonstrated quantitatively.

On the global scale, the situation is reversed; in diffuse growing cells, disrupting microtubules rarely fails to misalign microfibrils globally. In the shoot epidermis of many species, microfibril alignment cycles between transverse, oblique, and longitudinal, creating a layered, so-called polylamellate cell wall; when microtubules are removed, the layering stops and microfibrils appear to be deposited in a single orientation (Srivastava et al., 1977; Takeda and Shibaoka, 1981; Vian et al., 1982; Satiat-Jeunemaitre, 1984). Additionally, in the growth zone, cells with transverse alignment outnumber cells with oblique and longitudinal alignments; but when microtubules are removed, the three alignment classes become represented equally (Takeda and Shibaoka 1981; Iwata and Hogetsu, 1989). Studies like these support the idea

that microtubules are required to coordinate the alignment of microfibrils among cells; however the polylamellate condition makes interpreting the experiments difficult. Here, we took advantage of the Arabidopsis root, in which cell walls in the growth zone lack conspicuous lamellation (Zhu et al., 1998) and have consistently transverse microfibrils (Sugimoto et al., 2000), and show that disrupting microtubules can break down the global coherence of microfibril alignment.

How can the global alignment among microfibrils be governed by microtubules, short of mystical forces acting at a distance? We postulate that microfibrils are aligned locally by self-assembly and on a larger scale by cortical microtubules guiding the self-assembly process (Fig. 10). A potent role for self-assembly is reasonable, given that cellulose microfibrils are well ordered even when assembled in vitro (Whitney et al., 1995). In some cells, self-assembly may suffice entirely, for example root hairs with

helicoidal cell walls (Emons and Mulder, 1998); whereas in others, microtubule guidance may be paramount, for example in developing xylem, where parallel bands of a cellulose synthase subunit, observed as a green fluorescent protein-fusion, spread out immediately upon oryzalin treatment (Gardiner et al., 2003). However, most cells may lie between these extremes. In the Arabidopsis root, an intermediate level of microtubule guidance is suggested by several hours elapsing before microfibril alignment changes when microtubules are depolymerized completely (Sugimoto et al., 2003) or when they reorient from transverse to helical (Sugimoto et al., 2000). Microtubules could guide self-assembly by coordinating a membrane-spanning protein scaffold that binds nascent microfibrils and thereby influences their alignment (Baskin, 2001). If so, such a scaffold could be large and stable, and, once formed, might require only intermittent input from the cortical array for its alignment (Fig. 10).

Microtubules, Microfibrils, and Growth Anisotropy

Anisotropy of growth is characterized by the direction of maximal growth rate and by the difference between maximal and minimal growth rates, that is, the degree of anisotropy. The degree of anisotropy was hypothesized by Green (1964) to be proportional to the degree of alignment among microfibrils; that is, the more parallel cellulose microfibrils are laid down, the greater the difference between maximal and minimal expansion rates. This hypothesis was tested for the maize root, which grows more anisotropically under water deficit (Liang et al., 1997) and falsified; despite there being a more than 10-fold difference in the degree of anisotropy, there was no difference in microfibril alignment (Baskin et al., 1999). Likewise, decreased anisotropy occurs in several Arabidopsis mutants without detectable disorganization among microfibrils (Wiedemeier et al., 2002; Sugimoto et al., 2003).

We suggest that Green's hypothesis is valid, provided that it invokes the degree of alignment among microfibrils considered globally rather than locally (Fig. 10). An organ with a uniform tubular texture among microfibrils plausibly expands more anisotropically than one with patchy reinforcement. This resembles the situation in polylamellate stems where removal of microtubules causes swelling and an increase in the patchiness of microfibril orientation (Takeda and Shibaoka, 1981; Iwata and Hogetsu, 1989). In the work on roots cited above, apparently falsifying Green's hypothesis, none of the authors explicitly examined the variability of average microfibril orientation among cells, and a patchy distribution of locally well aligned cellulose may have been present. If so, this would be strong evidence that global microfibril alignment specifies the degree of anisotropy and that the role of microtubules in morphogenesis is to align microfibrils globally. Alternatively, the patchy microfibril orientation seen here may be
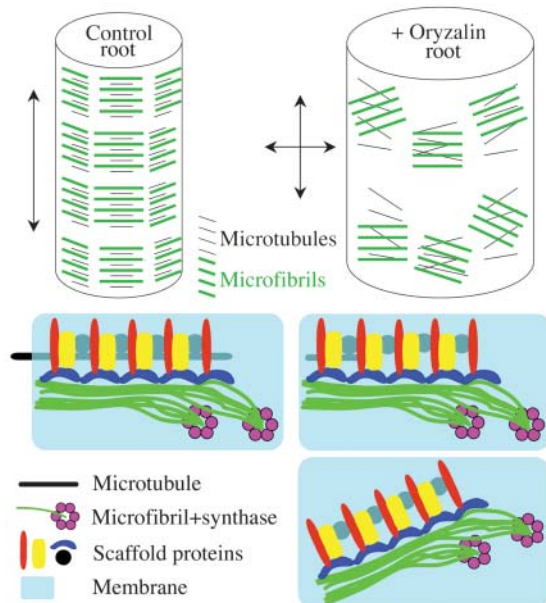

Figure 10. Relations between microtubules, microfibrils, and growth anisotropy. Top, Global level. On the left, the control root has a uniformly transverse alignment among microtubules and microfibrils, and highly anisotropic expansion (double-headed arrow to left). On the right, root treated with low oryzalin has partially disorganized microtubules and microfibrils that are well aligned locally but not globally. We hypothesize that the loss of uniform global alignment among microfibrils increases the rate of tangential expansion (double-headed arrows to left of root). Bottom, Model for the local level. On the left, the control, cortical microtubule organizes a scaffold of membrane proteins, some of which interact with the nascent microfibril to orient it. A second microfibril is oriented by self-assembly with respect to the first one. On the right, under oryzalin treatment, a short microtubule is able to maintain the scaffold's integrity, whereas at lower right, without a microtubule, the scaffold rotates as a whole and leads to locally coherent microfibril realignment. Viewed from the cell wall looking in, with microtubules and some of the scaffold lying beneath the membrane.

inconsequential, and, if so, then the reason for the reduced expansion anisotropy would have to be sought in an activity of microtubules other than aligning cellulose. Deciding between these alternatives is a challenge for future research.

MATERIALS AND METHODS

Material, Growth Conditions, and Treatments

Seeds of *Arabidopsis thaliana* L. (Heynh) ecotype Columbia were sterilized in dilute bleach and germinated on nutrient-solidified agar supplemented with 3% Suc in petri plates, sealed with air-permeable bandage tape, and seedlings were grown vertically under continuous yellow light (80 μmol m^{-2} s^{-1}) and constant temperature (19°C) for up to 10 d in a growth chamber, as described by Baskin and Wilson (1997). For experiments, 6- to 7-d-old seedlings were transplanted onto plates with the given concentration of inhibitor and returned to the growth chamber. There were three plates for each concentration, and each experiment was usually repeated three times.

Inhibitors were obtained from Sigma Chemical (St. Louis), except for the following: Propyzamide and oryzalin were from Chem Services (West Chester, PA), dithiopyr was a gift from Doug Sammonds (Monsanto, St. Louis), terbutol was a gift from Kevin Vaughn (Agricultural Research Service, Stonesville, MS), RH-4032 was a gift from David Young (Rohm and Haas, Philadelphia), and amiprophos-methyl was a gift from Dr. Carl Gregg (Bayer CropScience, Kansas City, MO). All compounds were dissolved in dimethyl sulfoxide (DMSO) except colchicines, which was dissolved in growth medium. Stocks were frozen between uses and diluted into measured quantities of melted agar at least 300-fold, and usually 1,000-fold. Control medium was given the maximal amount of DMSO used for a given dose-response curve.

Measurement of Growth

For measuring overall root elongation rate, plates containing seedlings were scored with a razor at the back of the plate at the position of the root tip, once per 24 h, and the plate was photocopied to end the experiment. The arc length of the root between marks, measured on a digitizing tablet interfaced to a computer running SigmaScan (Jandel Scientific, Corte Madera, CA), was divided by the time interval between marks. Root diameter was measured by imaging the roots at low magnification through a compound microscope directly on the agar plate, as described by Baskin and Wilson (1997).

The spatial profile of relative elongation rate was obtained as described by Beemster and Baskin (1998). Briefly, the root was dusted with fine graphite particles and allowed 1 h to recover. The petri dish containing seedlings was then clamped to the stage of a horizontal microscope, and images of the root captured via a CCD camera and a computer running the public domain NIH Image program (version 1.62; developed at the United States National Institutes of Health and available on the Internet at http://rsb.info.nih.gov/nih-image). Images were captured hourly for 4 h with the dish returned to the growth chamber between times. Five roots were imaged per treatment, each on a different petri dish. The positions of the marks at each time point were measured with NIH-Image. A separate image was also obtained by focusing at the median plane, from which was obtained the spatial profile of diameter and the distance between the root tip and the quiescent center. For each pair of images (five pairs), the measured displacements gave rise to a set of velocity-versus-position data and the five sets were pooled. A final velocity profile was obtained by a piece-wise, iterative polynomial fitting procedure that interpolated points at 25-μm intervals. The spatial profile of diameter was also smoothed and interpolated by the same algorithm. Relative tangential expansion rates were calculated from the spatial profiles of velocity and diameter (Silk and Abou Haidar, 1986; Liang et al., 1997). Longitudinal and tangential profiles were obtained for each root and then averaged over the roots in the treatment.

Examination of Microtubules and Microfibrils

Roots, treated as needed, were cryofixed as described by Baskin et al. (1996). Briefly, a root was mounted on a Formvar film supported on a wire
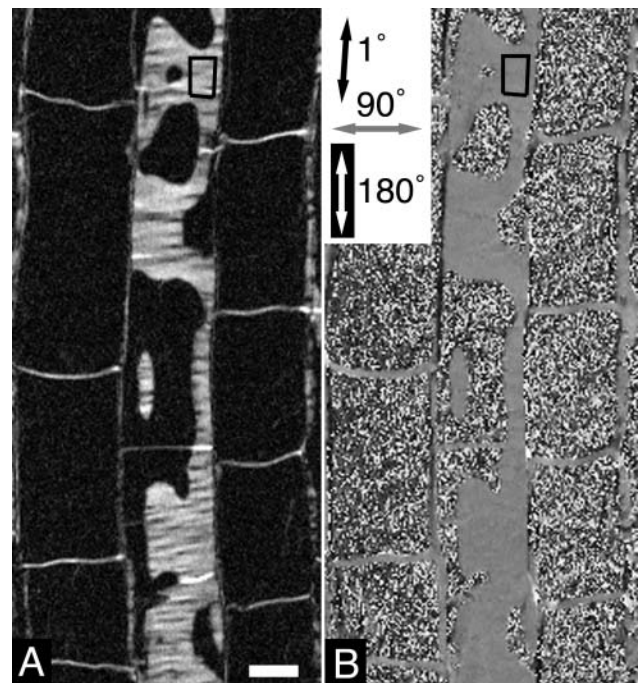

Figure 11. Polarized-light micrographs of a region of the root cortex illustrating the output of the LC-Pol Scope and the method of sampling. From a stack of four images (not shown) the instrument calculates digitally a pair of images in which the intensity of each pixel is proportional to (A) retardance and (B) azimuth of the optical axis of the birefringent element. Inset in the azimuth image shows the gray level coding. Boxes shown are typical of those used for measurement. The black (low retardance) throughout most cells in (A) reflects the absence of cell wall. Bar represents 10 μm.

loop and plunged into liquid propane at -180°C. Samples were then substituted in anhydrous ethanol for 2 d at -80°C, raised to room temperature, and embedded in butyl-methyl-methacrylate. Roots were sectioned longitudinally, at 2-μm thickness, with alternate sections collected for immunocytochemical detection of microtubules and polarized-light analysis of microfibrils. There were approximately 80 useful sections per root.

To detect microtubules, sections were stained with an antibody against sea urchin axonemal tubulin, and a CY-3-conjugated fluorescent secondary (Baskin and Wilson, 1997). Sections were examined on a fluorescence microscope (Axioplan; Zeiss, Thornwood, NY) and images captured with a CCD camera (VI-470; Optronics Engineering, Goleta, CA) interfaced to a computer running Image1/AT (Universal Imaging, West Chester, PA). Images with the clearest arrays were captured from each section, one to two per section, 50 to 60 images per root. In each image, the angle of 10 to 30 distinct microtubules was measured with Image1/AT. The distance of each image from the quiescent center was measured directly in medial sections. For the other sections, that distance was estimated by subtracting the distance between the quiescent center and the edge of the plastic section from the distance between the image and the section edge. Note that the angle made by the block face was measured and used to correct for the changing position of the section edge as a function of section depth.

To quantify microfibril organization, sections were examined with a polarized-light microscope (Interphako; Zeiss) equipped with a quantification device (LC Pol Scope; Cambridge Research Instruments, Cambridge, MA) based on digital video imaging (Oldenbourg and Mei, 1995). The LC Pol Scope calculates a retardance and an azimuth image (Fig. 11, A and B, respectively). In the retardance image, intensity is proportional to birefringent retardation (hence retardance); whereas, in the azimuth image, intensity is proportional to the angle defined by a reference line and the optical axis of the birefringent element (equivalent to extinction angle). An overlapping set of images was captured, spanning an entire section. Because cells are small in the meristem,

the apical-most two fields were imaged at 40× but all of the rest at 20×. Viewing the retardance image in NIH-Image, a box was placed on an area of cell wall parallel to the section plane and, simultaneously, a macro copied the box on the azimuth image (Fig. 11). The average pixel intensity of each box and the x, y coordinates were recorded. Boxes typically contained 100 to 200 pixels (approximately 5–10 μm^2 at 40×, 20–40 μm^2 at 20×), but ranged from 20 to 2,000 pixels. Virtually all suitable areas in the image were sampled (2–10 per image). Per treatment, four to five roots were sectioned, and five medial sections were sampled per root.

FESEM

Samples were prepared for FESEM as described by Sugimoto et al. (2000), with minor modifications. Samples were fixed in 4% (v/v) formaldehyde, 20 mM PIPES (pH 7.0), and 0.5 mM $CaCl_2$ for 2 h at room temperature, washed in 20 mM PIPES, and cryo-protected by incubating in 25% (v/v) DMSO in water for 30 min followed by 50% DMSO until cryo-sectioning at −115°C. After sectioning, cut-open roots were thawed in phosphate-buffered saline and encased between Formvar films on wire loops (Baskin and Wilson, 1997). Samples were treated with a 1:10 dilution of household bleach (0.525% [w/w] hypochlorite) for 30 min to remove cytoplasm, dehydrated in an ethanol series, critically point dried, sputter coated with platinum to a nominal thickness of 2 nm, and viewed in a FESEM (4700 S; Hitachi, Tokyo).

Orientation parameters were quantified from the FESEM images by means of a novel algorithm applied to the FFT, implemented as a plug-in for Image-J (v. 1.31e; developed by the United States National Institutes of Health and available on the Internet at http://rsb.info.nih.gov/ij) by Chris Coulon (GAIA Group, Novato, CA). In three dimensions (x, y, and I), the FFT can be likened to a mountain, with contour levels linking frequencies represented equally in the image. The algorithm analyzed the overall shape of the transform at a series of altitudes; the more circular the shape, the less well oriented the structures at those frequencies. A 256×256 pixel^2 (840×840 nm^2) region was chosen from each image and the FFT obtained. The transform was thresholded to generate a binary image, separating pixels containing power (black) from the background (white). An ellipse, a rough approximation to the shape of the transform, was fitted to the black pixels, and the major and minor axes recorded as well as the angle between the major axis and the vertical. Eccentricity (E) was calculated from the major (a) and minor (b) axes as:

$$E = \frac{\sqrt{a^2 - b^2}}{a}. \tag{1}$$

This was done iteratively, starting at the lowest threshold that gave a distinct shape, incrementing the threshold by five gray levels, and stopping when the area of the black pixels contained less than 200 pixels. The parameters for each threshold were assigned to the frequency of an average ellipse radius, $(a + b)/4$, and this frequency was converted to a distance by dividing it into the total width of the transform (256 pixels).

LITERATURE CITED

Baskin TI (2001) On the alignment of cellulose microfibrils by cortical microtubules: a review and a model. Protoplasma 215: 150–171

Baskin TI, Beemster GTS (1998) On the "postmitotic isodiametric growth zone" in roots. In HE Flores, J Lynch, D Eissenstat, eds, Radical Biology, Advances and Perspectives on the Function of Plant Roots. American Society of Plant Physiologists, Rockville MD, pp 23–33

Baskin TI, Meekes HTHM, Liang BM, Sharp RE (1999) Regulation of growth anisotropy in well-watered and water-stressed maize roots. II. Role of cortical microtubules and cellulose microfibrils. Plant Physiol 119: 681–692

Baskin TI, Miller DD, Vos JW, Wilson JE, Hepler PK (1996) Cryofixing single cells and multicellular specimens enhances structure and immunocytochemistry for light microscopy. J Microsc 182: 149–161

Baskin TI, Wilson JE (1997) Inhibitors of protein kinases and phosphatases alter root morphology and disorganize cortical microtubules. Plant Physiol 113: 493–502

Baskin TI, Wilson JE, Cork A, Williamson RE (1994) Morphology and microtubule organization in arabidopsis roots exposed to oryzalin or taxol. Plant Cell Physiol 35: 935–942

Beemster GTS, Baskin TI (1998) Analysis of cell division and elongation underlying the developmental acceleration of root growth in Arabidopsis thaliana. Plant Physiol 116: 1515–1526

Bichet A, Desnos T, Turner S, Grandjean O, Höfte H (2001) BOTERO1 is required for normal orientation of cortical microtubules and anisotropic cell expansion in Arabidopsis. Plant J 25: 137–148

Burk DH, Ye Z-H (2002) Alteration of oriented deposition of cellulose microfibrils by mutation of a katanin-like microtubule-severing protein. Plant Cell 14: 2145–2160

Cleary AL, Hardham AR (1988) Depolymerization of microtubule arrays in root tip cells by oryzalin and their recovery with modified nucleation patterns. Can J Bot 66: 2353–2366

Emons AMC, Derksen J, Sassen MMA (1992) Do microtubules orient plant cell wall microfibrils? Physiol Plant 84: 486–493

Emons AMC, Mulder BM (1998) The making of the architecture of the plant cell wall: how cells exploit geometry. Proc Natl Acad Sci USA 95: 7215–7219

Ennis WB Jr (1948) Some cytological effects of O-isopropyl N-phenyl carbamate upon Avena. Am J Bot 35: 15–21

Erickson RO (1966) Relative elemental rates and anisotropy of growth in area: a computer programme. J Exp Bot 17: 390–403

Erickson RO (1980) Microfibrillar structure of growth plant cell walls. In WM Getz, ed, Mathematical Modelling [sic] in Biology and Ecology, Lecture Notes in Biomathematics, Vol 33. Springer-Verlag, Berlin, pp 192–212

Galatis B, Apostolakos P (1991) Patterns of microtubule reappearance in root cells of Vigna sinensis recovering from a colchicine treatment. Protoplasma 160: 131–143

Gardiner JC, Taylor NG, Turner SR (2003) Control of cellulose synthase complex localization in developing xylem. Plant Cell 15: 1740–1748

Green PB (1964) Cell walls and the geometry of plant growth. Brookhaven Symp Biol 16: 203–217

Green PB (1976) Growth and cell pattern formation on an axis: critique of concepts, terminology, and modes of study. Bot Gaz 137: 187–202

Green PB (1980) Organogenesis: a biophysical view. Annu Rev Plant Physiol 31: 51–82

Hardham AR, Gunning BES (1980) Some effects of colchicine on microtubules and cell division in roots of Azolla pinnata. Protoplasma 102: 31–51

Hepler PK, Newcomb EH (1964) Microtubules and fibrils in the cytoplasm of Coleus cells undergoing secondary wall deposition. J Cell Biol 20: 529–533

Himmelspach R, Williamson RE, Wasteneys GO (2003) Cellulose microfibril alignment recovers from DCB-induced disruption despite microtubule disorganization. Plant J 36: 565–575

Hoffman JC, Vaughn KC (1994) Mitotic disrupter herbicides act by a single mechanism but vary in efficacy. Protoplasma 179: 16–25

Holmsen JD, Hess FD (1985) Comparison of the disruption of mitosis and cell plate formation in oat roots by DCPA, colchicine, and propham. J Exp Bot 36: 1504–1513

Hugdahl JD, Morejohn LC (1993) Rapid and reversible high affinity binding of the dinitroaniline herbicide oryzalin to tubulin from Zea mays L. Plant Physiol 102: 725–740

Iwata K, Hogetsu T (1989) Orientation of wall microfibrils in Avena coleoptiles and mesocotyls and in Pisum epicotyls. Plant Cell Physiol 30: 749–757

Kwiatkowska D, Dumais J (2003) Growth and morphogenesis at the vegetative shoot apex of Anagallis arvensis L. J Exp Bot 54: 1585–1595

Ledbetter MC, Porter KR (1963) A "microtubule" in plant cell fine structure. J Cell Biol 19: 239–250

Liang BM, Dennings AM, Sharp RE, Baskin TI (1996) Consistent handedness of micro-tubule helical arrays in maize and arabidopsis primary roots. Protoplasma **190:** 8–15

Liang BM, Sharp RE, Baskin TI (1997) Regulation of growth anisotropy in well-watered and water-stressed maize roots I Spatial distribution of longitudinal, radial, and tangential expansion rates. Plant Physiol **115:** 101–111

Ma Z, Baskin TI, Brown KM, Lynch JP (2003) Regulation of root elongation under phosphorus stress involves changes in ethylene responsiveness. Plant Physiol **131:** 1381–1390

Mark RE (1967) Cell Wall Mechanics of Tracheids. Yale University Press, New Haven, CT, pp 1–26

Mineyuki Y (1999) The preprophase band of microtubules: its function as a cytokinetic apparatus in higher plants. Int Rev Cytol **187:** 1–49

Oldenbourg R, Mei G (1995) New polarized light microscope with precision universal compensator. J Microsc **180:** 140–147

Preston RD (1982) The case for multinet growth in growing walls of plant cells. Planta **155:** 356–363

Satiat-Jeunemaitre B (1984) Experimental modifications of the twisting and rhythmic pattern in the cell walls of maize coleoptile. Biol Cell **51:** 373–380

Sharp RE, Silk WK, Hsiao TC (1988) Growth of the maize primary root at low water potentials I Spatial distribution of expansive growth. Plant Physiol **87:** 50–57

Silk WK, Abou Haidar S (1986) Growth of the stem of *Pharbitis nil*: analysis of longitudinal and radial components. Physiol Veg **24:** 109–116

Smith LG, Gerttula SM, Han S, Levy J (2001) TANGLED1: a microtubule binding protein required for the spatial control of cytokinesis in Maize. J Cell Biol **152:** 231–236

Srivastava LM, Sawhney VK, Bonettmaker M (1977) Cell growth, wall deposition, and correlated fine structure of colchicine-treated lettuce hypocotyl cells. Can J Bot **55:** 902–917

Sugimoto K, Himmelspach R, Williamson RE, Wasteneys GO (2003) Mutation or drug-dependent microtubule disruption causes radial swelling without altering parallel cellulose microfibril deposition in arabidopsis root cells. Plant Cell **15:** 1414–1429

Sugimoto K, Williamson RE, Wasteneys GO (2000) New techniques enable comparative analysis of microtubule orientation, wall texture, and growth rate in intact roots of arabidopsis. Plant Physiol **124:** 1493–1506

Taiz L (1984) Plant cell expansion: regulation of cell wall mechanical properties. Annu Rev Plant Physiol **35:** 585–657

Takeda K, Shibaoka H (1981) Effects of gibberellin and colchicine on microfibril arrangement in epidermal cell walls of *Vigna angularis* Ohwi et Ohashi epicotyls. Planta **151:** 393–398

Thitamadee S, Tuchihara K, Hashimoto T (2002) Microtubule basis for left-handed helical growth in Arabidopsis. Nature **417:** 193–196

van der Weele CM, Spollen WG, Sharp RE, Baskin TI (2000) Growth of *Arabidopsis thaliana* seedlings under water deficit studied by control of water potential in nutrient-agar media. J Exp Bot **51:** 1555–1562

Vaughn KC, Lehnen LP Jr (1991) Mitotic disrupter herbicides. Weed Sci **39:** 450–457

Vian B, Mosiniak M, Reis D, Roland J-C (1982) Dissipative process and experimental retardation of the twisting in the growing plant cell wall: effect of ethylene-generating agent and colchicine: a morphogenetic revaluation. Biol Cell **46:** 301–310

Wasteneys GO, Galway ME (2003) Remodeling the cytoskeleton for growth and form: an overview with some new views. Annu Rev Plant Biol **54:** 691–722

Whitney SEC, Brigham JE, Darke AH, Grant Reid JS, Gidley MJ (1995) In vitro assembly of cellulose/xyloglucan networks: ultrastructural and molecular aspects. Plant J **8:** 491–504

Wiedemeier AMD, Judy-March JE, Hocart CH, Wasteneys GO, Williamson RE, Baskin TI (2002) Mutant alleles of arabidopsis *RADIALLY SWOLLEN 4* and *RSW7* reduce growth anisotropy without altering the transverse orientation of cortical microtubules or cellulose microfibrils. Development **129:** 4821–4830

Williamson RE (1991) Orientation of cortical microtubules in interphase plant cells. Int Rev Cytol **129:** 135–206

Young DH, Lewandowski VT (2000) Covalent binding of the benzamide RH-4032 to tubulin in sususpension-cultured tobacco cells and its application in a cell-based competitive-binding assay. Plant Physiol **124:** 115–124

Zhu T, Lucas WJ, Rost TL (1998) Directional cell-to-cell communication in the Arabidopsis root apical meristem I. An ultrastructural and functional analysis. Protoplasma **203:** 35–47